

Towards weighing the condensation energy to ascertain the Archimedes force of vacuum

Enrico Calloni,^{*} Martina De Laurentis,[†] Rosario De Rosa,[‡] Fabio Garufi,[§] and Luigi Rosa[¶]
*Università di Napoli Federico II, Dipartimento di Fisica, Complesso Universitario di Monte S. Angelo,
 Via Cintia Edificio 6, 80126 Napoli, Italy and Istituto Nazionale di Fisica Nucleare, Sezione di Napoli,
 Complesso Universitario di Monte S. Angelo, Via Cintia Edificio 6, 80126 Napoli, Italy*

Luciano Di Fiore[‡] and Giampiero Esposito^{**}
*Istituto Nazionale di Fisica Nucleare, Sezione di Napoli, Complesso Universitario di Monte S. Angelo,
 Via Cintia Edificio 6, 80126 Napoli, Italy*

Carlo Rovelli^{††}
*Aix Marseille Université CNRS, CPT, UMR 7332, 13288 Marseille, France
 and Université de Toulon, CNRS, CPT, UMR 7332, 83957 La Garde, France*

Paolo Ruggi^{‡‡}
European Gravitational Observatory (EGO), I-56021 Cascina (Pi), Italy

Francesco Tafuri^{§§}
*Dipartimento Ingegneria dell'Informazione, Seconda Università di Napoli, I-81031 Aversa (CE), Italy
 (Received 27 January 2014; published 10 July 2014)*

The force exerted by the gravitational field on a Casimir cavity in terms of Archimedes force of vacuum is discussed, the force that can be tested against observation is identified, and it is shown that the present technology makes it possible to perform the first experimental tests. The use of suitable high- T_c superconductors as modulators of Archimedes force is motivated. The possibility is analyzed of using gravitational wave interferometers as detectors of the force, transported through an optical spring from the Archimedes vacuum force apparatus to the gravitational interferometer test masses to maintain the two systems well separated. The use of balances to actuate and detect the force is also analyzed, the different solutions are compared, and the most important experimental issues are discussed.

DOI: [10.1103/PhysRevD.90.022002](https://doi.org/10.1103/PhysRevD.90.022002)

PACS numbers: 04.80.Cc, 07.05.Fb

I. INTRODUCTION

One of the striking and long-standing problems of fundamental physics is the irreconcilability among the two main theories of last century, general relativity and quantum theory. A manifestation of this tension is the value that quantum field theory attributes to the vacuum energy density, enormously larger than the value constrained from general relativity by considering the radius of our Universe. This problem, known as the cosmological constant problem [1], has been faced over the past decades with profound theoretical investigations, following also the evolution of the most important quantum gravity theories, like string theories, loop quantum gravity,

and many others [2–4]. None of the theoretical efforts has so far succeeded in finding a consensual solution, so that it is still questionable whether vacuum energy does interact with gravity, and what its contribution is to the cosmological constant [5,6]. In spite of the common belief by the scientific community in the existence of an interaction between vacuum energy and gravity, not a single experimental test of this interaction exists.

About a decade ago, it was pointed out that a possible way to verify the interaction of vacuum fluctuations with gravity was to weigh a (suitably realized, layered) rigid Casimir cavity [7]. At that time it was yet unclear whether Casimir energy could be modulated in a rigid cavity. Furthermore, the most important macroscopic detectors of exceedingly small forces, the gravitational wave detectors with which we compared our force, were still under construction. Nowadays, thanks to many activities in the various fields mentioned, the situation has been remarkably improved so that it is possible to step from the initial idealistic experiment to a road map towards the measurement of the effect.

^{*}enrico.calloni@na.infn.it

[†]martina.delarentis@na.infn.it

[‡]rosario.derosa@na.infn.it

[§]fabio.garufi@na.infn.it

[¶]luigi.rosa@na.infn.it

^{**}giampiero.esposito@na.infn.it

^{††}rovelli@cpt.univ-mrs.fr

^{‡‡}ruggi@ego-gw.it

^{§§}francesco.tafuri@na.infn.it

The paper is organized as follows. In Sec. II the theory of the experiment is recalled and discussed to clearly identify the measured quantity. In Sec. III the need for superconductors as actuators of modulation of the Casimir stress-energy tensor is proposed. In particular, the use of High- T_c superconductors is pointed out. The first part of the section is devoted to describe the theory and method of the evaluation of vacuum energy in the well-established case of type-I superconductors. This makes it possible to discuss, in the second part, the hypothesis and approximations assumed for the case of type-II superconductors. Finally, the force exerted by gravity on a multilayer superconductor Casimir-cavity system will be considered. In Sec. IV the expected force is compared with the sensitivity of advanced gravitational wave detectors: an optical technique to link the force on the Casimir-test mass with the test mass of gravitational wave detectors is presented, and the noises are discussed in detail. In Sec. V the possibility to perform the measurement in the superconductors' transition-favored low-frequency regime is discussed by analyzing the use of a suitable seismic isolated balance. The comparison of the two experimental ways is discussed in light of the most critical experimental issues.

II. THEORETICAL ASPECTS

Let us consider a rigid Casimir cavity in a weak gravitational field, like the one, for instance, of a laboratory at rest on the surface of the Earth. To first order, the reference system is the Fermi system for which, neglecting rotations, one can write the line element as [7–9]

$$ds^2 = -(1 + 2A_j x^j)(dx^0)^2 + \delta_{jk} dx^j dx^k + O_{\alpha\beta}(|x^j|^2) dx^\alpha dx^\beta. \quad (2.1)$$

The term $c^2 \vec{A}$, c being the speed of light, is the observer's acceleration with respect to the local freely falling frame. It has components $(0, 0, |\vec{g}|)$, where g is the gravitational acceleration. The term $-2A_j x^j$ is proportional to the distance along the acceleration direction; x^3 , which we also denote by z , is positive in the upwards direction.

The force exerted by the gravitational field on a rigid Casimir cavity, with plates of proper area \mathcal{A} , separated by the proper distance a and placed orthogonal to the gravitational acceleration \vec{g} , has been calculated in different ways [7–13]. To clarify the proposed measurement we briefly recall the main points.

When a force is applied to a stressed body it is in general expected that also the spatial components of the stress-energy tensor contribute to the mass. This was first shown by Einstein [14] and it is reported, for example, in Ref. [15], Eqs. (5.53) and (5.54) where one considers a stressed body in a locally inertial frame that is accelerated with $a^k = \frac{dv^k}{dt}$. The mass density is described by the tensor $m^{ik} = T^{\hat{0}\hat{0}} \delta^{ik} + T^{\hat{i}\hat{k}}$, where the hat over the indices denotes

the stress tensor in the rest frame of the medium and the force is defined as $F^j = \sum_k m^{jk} \frac{dv^k}{dt}$. In analogy, since the Casimir cavity is a stressed body, one could expect that the measurement of its weight would end in measuring the stressed-body mass and not simply the mass associated with the $T^{\hat{0}\hat{0}}$ term. In this case, considering that the rest frame stress-energy tensor of a Casimir cavity is given by Ref. [16],

$$\langle T^{\mu\nu} \rangle = \frac{\pi^2 \hbar c}{180 a^4} \left(\frac{1}{4} \eta^{\mu\nu} - \hat{h}^\mu \hat{h}^\nu \right), \quad (2.2)$$

where $\hat{h}^\mu = (0, 0, 0, 1)$ is the unit spacelike 4-vector orthogonal to the plates' surface; one could expect that the cavity of volume $V = a\mathcal{A}$, placed with plates parallel to the Earth's surface, would have a mass $m_h = V(T^{\hat{0}\hat{0}} + T^{\hat{3}\hat{3}}) = 4a\mathcal{A}T^{\hat{0}\hat{0}} = 4 \frac{E_{\text{cas}}}{c^2}$, where $E_{\text{cas}} = -\mathcal{A} \frac{\hbar \pi^2 c}{720 a^3}$ is the energy of the system, the Casimir energy. This would result in the force $\vec{F}_h = 4 \frac{E_{\text{cas}}}{c^2} \vec{g}$ exerted by the gravitational field on the cavity. Although this result is compliant with general relativity, it is nevertheless somewhat surprising, because usually one is accustomed to attributing, to a body of rest energy E , the weight $\vec{F} = \frac{E}{c^2} \vec{g}$. The surprise is indeed correct, because in fact the previous result does not correspond to the actual force measured in a weight experiment where the cavity is rigid and hanged at a single fixed point (or placed on a plate of a balance). To correctly evaluate the force measured in these cases, the force densities acting on the various points must be redshifted: Refs. [8] and in particular [13] clarified that, if the total force acting on an extended body is defined as the sum of redshifted force densities, the mass is independent of the spatial stress-energy tensor.

To very well clarify the measured quantity, we consider the forces on each plate, expanded to first order in $\epsilon \equiv 2 \frac{ga}{c^2}$, derived in Ref. [9]. In that work the regularized and renormalized energy-momentum tensor $T^{\mu\nu}$ has been obtained from the Hadarmard Green function of a Casimir apparatus in a weak gravitational field. The forces on the plates are the components of the resulting stress-energy tensor and, for the z direction, have been evaluated as (hereafter Q_2 refers to the upper plate and Q_1 to the lower plate)

$$\vec{f}_{Q_2} \approx -\frac{\pi^2 \mathcal{A} \hbar c}{240 a^4} \left[1 - \frac{g}{c^2} \left(\frac{2}{3} a \right) \right] \hat{z}, \quad (2.3)$$

while for the lower plate we get

$$\vec{f}_{Q_1} \approx \frac{\pi^2 \mathcal{A} \hbar c}{240 a^4} \left[1 + \frac{g}{c^2} \left(\frac{2}{3} a \right) \right] \hat{z}. \quad (2.4)$$

The mere addition of such forces (as it might be obtained by independently measuring the forces acting on the two plates of a nonrigid system) would lead to the quantity f_{ind} equal to

$$\vec{f}_{\text{ind}} = \vec{f}_{Q_1} + \vec{f}_{Q_2} \approx \left(\frac{|E_{\text{cas}}|}{c^2}(\mathbf{g}) + F_{\text{cas}}\delta\phi \right) \hat{z}, \quad (2.5)$$

where $P_{\text{cas}} = \mathcal{A} \frac{\hbar\pi^2 c}{240a^4}$ is the Casimir pressure, where $F_{\text{cas}} = \mathcal{A} P_{\text{cas}}$ is the Casimir force, and where $\frac{ga}{c^2} = \delta\phi$ has been explicitly written as the variation of the gravitational potential on passing from the lower to the upper plate. By some algebra Eq. (2.5) reads as $\vec{f}_{\text{ind}} = 4 \frac{E_{\text{cas}}}{c^2} \vec{g}$ corresponding to the case of the nonrigid cavity. Interestingly, Eq. (2.5) is the sum of two contributions: the vacuum weight part $\frac{E_{\text{cas}}}{c^2} \mathbf{g}$ and the Casimir pressure difference, multiplied by the surface, $\mathcal{A} P_{\text{cas}} \delta\phi$, on passing from one plate to the other.

$$\begin{aligned} \vec{F} = \vec{f}_{Q_2} + r_{Q_2}(Q_1)\vec{f}_{Q_1}^{(C)} &\approx F_{\text{cas}} \left\{ - \left[1 - \frac{\mathbf{g}}{c^2} \left(\frac{2}{3}a \right) \right] + \left[1 - \frac{\mathbf{g}}{c^2} a \right] \left[1 + \frac{\mathbf{g}}{c^2} \left(\frac{2}{3}a \right) \right] \right\} \hat{z} \\ &\approx \frac{1}{3} \frac{ga}{c^2} F_{\text{cas}} \hat{z} = \frac{E_{\text{cas}}}{c^2} \vec{g}. \end{aligned} \quad (2.6)$$

This condition is the case of the experiment here proposed, where a rigid (multi)cavity system is suspended in the gravitational field of the earth. This is the force that must be tested against observation, and it is in full agreement with the expectation of the equivalence principle. It is directed upwards, and it is equal to the weight of the modes of the vacuum that are removed from the cavity. Therefore it can be interpreted as an Archimedes buoyancy force in vacuum.

III. SUPERCONDUCTORS

The measurement of the effect cannot be performed statically. This would make it necessary to compare the weight of the assembled cavity with the sum of the weights of its individual parts, which cannot be performed. Thus, it becomes necessary to modulate the Casimir energy contained in the cavity to be weighed, so as to perform the measurement in a region of frequency where the macroscopic detectors of small forces have good sensitivity. Furthermore, to actually perform the measurement, the cavity should be a rigid body, so as to be weighed as a whole, and consisting of a multilayer of many cavities to enhance the effect. A key point in modulation is that the energy supplied to the system should be at most of the same order of magnitude of the Casimir energy modulation; otherwise it will be extremely difficult to recover the Casimir contribution to the weight. Some recent techniques, as an example, even if very interesting for studying the Casimir force [19,20], cannot be applied in our case because the efficiency is very low: only a few parts in a billion of the energy supplied to the system are converted in Casimir energy variation.

One possible way is to use superconductors. To show the foundation of the theory and method of evaluation of vacuum energy, in the first part of the section we show

This difference in pressure is physical, and it implies the redshifting of vacuum density in the gravitational field. It is similar to the Tolman-Ehrenfest effect [17,18] where the same dependence is found in the temperature of a gas at equilibrium in a gravitational field.

In the measurement we are interested in, however, the plates are weighed by acting on one and the same point, i.e., the suspension point of the rigid Casimir apparatus. In this case, as shown in Ref. [13], the gravitational redshift must be taken into account when summing the force to obtain the total force acting on the body. By redshifting the force up to the common point Q_2 , the total force is given by (recall that \hat{z} and \vec{g} have the opposite direction)

some known results in case of type-I superconductors. This will allow one, in the second part of the section, to discuss both the motivation for using type-II superconductors and the present limits and approximations in evaluating the vacuum energy in that case. To fix the ideas consider a double cavity, consisting of two identical plane parallel mirrors, made of a nonsuperconducting and nonmagnetic metal, between which a plane superconducting film of thickness D (order of few nanometers) is placed, separated by a nonconducting material gap of equal width L (order few nanometers) from the two mirrors, as in Fig. 1. If the superconductor is of type I, for any temperature T lower than the transition temperature T_c the transition Gibbs free energy ΔF can be written as the sum of the condensation energy $\mathcal{E}(T)$ and the variation of Casimir energy $\Delta E_{\text{cas}}(T)$,

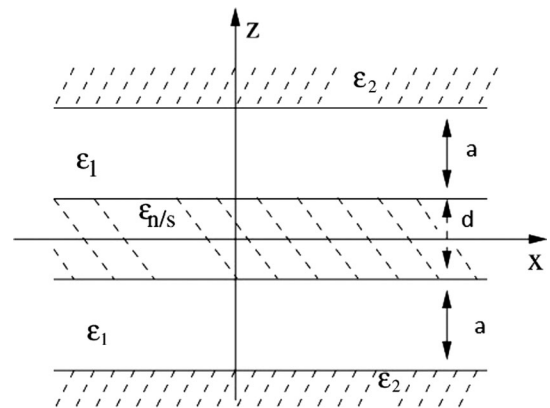


FIG. 1. Five-layer cavity: a thin superconducting film of thickness d is placed between two thick metallic slabs, which constitute the plates of the cavity. The gaps of width a that separate the film from the plates are filled with insulating material.

$$\Delta F = \mathcal{E}(T) + \Delta E_{\text{cas}}(T). \quad (3.1)$$

In writing these equations, we have exploited the fact that all quantities referring to the film, like the penetration depth, condensation energy, etc., are not affected by virtual photons in the surrounding cavity. This is a very good approximation, since the leading effect of radiative corrections is a small renormalization of the electron mass as discussed in

$$\Delta E_{\text{cas}}^0(a, d) = A \frac{\hbar}{2} \int \frac{dk_1 dk_2}{(2\pi)^2} \left\{ \sum_p (\omega_{\mathbf{k}_\perp, p}^{(n, \text{TM})} + \omega_{\mathbf{k}_\perp, p}^{(n, \text{TE})}) - \sum_p (\omega_{\mathbf{k}_\perp, p}^{(s, \text{TM})} + \omega_{\mathbf{k}_\perp, p}^{(s, \text{TE})}) \right\}, \quad (3.2)$$

where $A \gg a^2$ is the area of the cavity, $\mathbf{k}_\perp = (k_1, k_2)$ denotes the two-dimensional wave vector in the xy plane, while $\omega_{\mathbf{k}_\perp, p}^{(n/s, \text{TM})}$ ($\omega_{\mathbf{k}_\perp, p}^{(n/s, \text{TE})}$) denote the proper frequencies of the TM (TE) modes, in the n/s states of the film, respectively.

By exploiting the Cauchy integral formula, and by subtracting the contribution corresponding to infinite separation a (for details, we refer the reader to Chap. 4 of the first source of Ref. [19]), one can rewrite the renormalized sums in Eq. (8) as integrals over complex frequencies $i\zeta$,

$$\begin{aligned} & \left(\sum_p \omega_{\mathbf{k}_\perp, p}^{(n, \text{TM})} - \sum_p \omega_{\mathbf{k}_\perp, p}^{(s, \text{TM})} \right)_{\text{ren}} \\ &= \frac{1}{2\pi} \int_{-\infty}^{\infty} d\zeta \left(\log \frac{\Delta_n^{(1)}(i\zeta)}{\tilde{\Delta}_{n\infty}^{(1)}(i\zeta)} - \log \frac{\Delta_s^{(1)}(i\zeta)}{\tilde{\Delta}_{s\infty}^{(1)}(i\zeta)} \right), \end{aligned} \quad (3.3)$$

where $\Delta_{n/s}^{(1)}(i\zeta)$ is the expression in Eq. (4.7) of Ref. [19] (evaluated for $\epsilon_0 = \epsilon_{n/s}$) and $\tilde{\Delta}_{n/s\infty}^{(1)}(i\zeta)$ denotes the asymptotic value of $\Delta_{n/s}^{(1)}(i\zeta)$ in the limit $a \rightarrow \infty$ (corresponding to the limit $d \rightarrow \infty$ with the notation of Ref. [19]). A similar expression can be written for the TE modes, which involves the quantity $\Delta_{n/s}^{(2)}(i\zeta)$ defined in Eq. (4.9) of [19]. Upon inserting Eq. (3.3), and the analogous expression for TE

Refs. [21,22]. The variation of Casimir energy at the transition can be calculated starting from the theory of Casimir energy in stratified media, derived in Ref. [19]. We consider first the $T = 0$ case. The Casimir energy is given by the sum over the cavity modes; the wave numbers k are discretized in the z direction (orthogonal to the plates) and continuous in the parallel directions (the xy plane). The variation of Casimir energy $\Delta E_{\text{cas}}^0(a, d)$ at the transition can then be written as

modes, into Eq. (3.2) one gets the following expression for the (renormalized) variation $\Delta E^{(C)}(a, d)$ of the Casimir energy:

$$\Delta E_{\text{cas}} = A \frac{\hbar}{2} \int \frac{d\mathbf{k}_\perp}{(2\pi)^2} \int_{-\infty}^{\infty} \frac{d\zeta}{2\pi} \left(\log \frac{Q_n^{\text{TE}}}{Q_s^{\text{TE}}} + \log \frac{Q_n^{\text{TM}}}{Q_s^{\text{TM}}} \right), \quad (3.4)$$

where we set

$$Q_I^{(\text{TM/TE})}(\zeta) \equiv \frac{\Delta_I^{(1/2)}(i\zeta)}{\tilde{\Delta}_{I\infty}^{(1/2)}(i\zeta)}, \quad I = n, s. \quad (3.5)$$

The $d\mathbf{k}_\perp$ integration can be reexpressed through the dp integration by means of the standard formula $k_\perp^2 = (p^2 - 1)\zeta^2/c^2$. The above expression for $\Delta E_{\text{cas}}(a, d)$ turns therefore into

$$\Delta E_{\text{cas}} = \frac{\hbar A}{4\pi^2 c^2} \int_1^\infty p dp \int_0^\infty d\zeta \zeta^2 \left(\log \frac{Q_n^{\text{TE}}}{Q_s^{\text{TE}}} + \log \frac{Q_n^{\text{TM}}}{Q_s^{\text{TM}}} \right), \quad (3.6)$$

where the coefficients $Q_I^{(\text{TM/TE})}$ read as

$$\begin{aligned} Q_I^{\text{TE/TM}}(\zeta, p) &= \frac{(1 - \Delta_{1I}^{\text{TE/TM}} \Delta_{12}^{\text{TE/TM}} e^{-2\zeta K_1 L/c})^2 - (\Delta_{1I}^{\text{TE/TM}} - \Delta_{12}^{\text{TE/TM}} e^{-2\zeta K_1 L/c})^2 e^{-2\zeta K_I D/c}}{1 - (\Delta_{1I}^{\text{TE/TM}})^2 e^{-2\zeta K_I D/c}}, \\ \Delta_{jl}^{\text{TE}} &= \frac{K_j - K_l}{K_j + K_l}, \quad \Delta_{jl}^{\text{TM}} = \frac{K_j \epsilon_l(i\zeta) - K_l \epsilon_j(i\zeta)}{K_j \epsilon_l(i\zeta) + K_l \epsilon_j(i\zeta)}, \\ K_j &= \sqrt{\epsilon_j(i\zeta) - 1 + p^2}, \quad I = n, s; \quad j, l = 1, 2, n, s. \end{aligned} \quad (3.7)$$

The generalization of these formulas to the case of finite temperature T can be done with the well-known technique of Matsubara frequencies. This consists in replacing in Eq. (3.4) the integration $\int d\zeta/2\pi$ by the summation $kT/\hbar \sum_l$ over the Matsubara frequencies $\zeta_l = 2\pi l/\beta$, where $\beta = \hbar/(kT)$. This leads to the following expression for the variation $\Delta E_{\text{cas}}(T)$ of Casimir free energy:

$$\Delta E_{\text{cas}}(T) = A \frac{kT}{2} \sum_{l=-\infty}^{\infty} \int \frac{d\mathbf{k}_\perp}{(2\pi)^2} \left(\log \frac{Q_n^{\text{TE}}}{Q_s^{\text{TE}}} + \log \frac{Q_n^{\text{TM}}}{Q_s^{\text{TM}}} \right). \quad (3.8)$$

Equations (3.6)–(3.8) involve the dielectric functions $\epsilon(i\zeta)$ of the various layers evaluated at imaginary frequencies $i\zeta$.

For the outermost metal plates, the Drude model for the dielectric function can be used,

$$\epsilon_D(\omega_p) = 1 - \frac{\Omega^2}{\omega(\omega + i\gamma)}, \quad (3.9)$$

where Ω_p is the plasma frequency and $\gamma = 1/\tau$, with τ the relaxation time. We denote by Ω_{p2} and τ_{p2} the values of these quantities for the outer plates. As is well known, the Drude model provides a very good approximation in the low-frequency range $\omega \approx 2kT_c/\hbar \approx 10^{11}-10^{12}$ rad/sec, which is involved in the computation of $\Delta E_{\text{cas}}(T)$. The continuation of Eq. (3.9) to the imaginary axis is, of course, straightforward and gives

$$\epsilon_D(i\zeta) = 1 + \frac{\Omega^2}{\zeta(\zeta + \gamma)}. \quad (3.10)$$

For the insulating layers, a constant dielectric function can be taken, as a good approximation [19,22], equal to the static value,

$$\epsilon_1(\omega) = \epsilon_1(0). \quad (3.11)$$

As far as the film is concerned, in case of type-I superconductors, the Drude expression, Eq. (3.9), can be used in the normal state, with appropriate values for the plasma frequency Ω_n and the relaxation time τ_n .

In the superconducting state, the technical details are more involved, but the theory is still based on firm ground. The real part of the conductivity $\sigma(\omega)$ has a semiexplicit form, derived by the Bardeen-Cooper-Schrieffer theory, that we report in Appendix A, and it shows the lowering of the absorption component for frequencies $\hbar\omega$ less than the condensation energy gap $\Delta(T)$ and tends to the Drude expression for higher frequencies. (See Appendix A for details.)

From the real part of the conductivity $\sigma'(\omega)$ one can obtain the imaginary part of the dielectric function $\epsilon''(\omega)$ with the standard relation

$$\epsilon''(\omega) = \frac{4\pi}{\omega} \sigma'(\omega). \quad (3.12)$$

Last, from the dispersion relation, the dielectric function at imaginary frequency can be found in the form

$$\epsilon_s(i\zeta) - 1 = \frac{2}{\pi} \int_0^\infty d\omega \frac{\omega \epsilon''_s(\omega)}{\zeta^2 + \omega^2}. \quad (3.13)$$

With this recipe it is possible to calculate the variation of free energy at the transition. In general, for a stand-alone superconductor, not being part of a Casimir cavity, the free energy variation at the transition is equal to the source magnetic energy necessary to destroy the superconductivity,

$$\frac{V}{2\mu_0} \left(\frac{B_{c\parallel}(T)}{\rho} \right)^2 = \mathcal{E}_{\text{cond}}(T), \quad (3.14)$$

where V is the volume of the superconducting film. The term ρ takes into account that for a thin film, of thickness $d \ll \lambda, \xi$ (with λ the penetration depth and ξ the correlation length), placed in a parallel magnetic field, expulsion of the magnetic field is incomplete, and consequently the critical field increases from B_c (the bulk value) to $B_{c\parallel}$. Following the Ginzburg-Landau theory, the transition is a second-order transition (no latent heat) and as B approaches $B_{c\parallel}$ the order parameter (energy gap, “number of superconducting electrons,” or Ginzburg-Landau ψ function) approaches zero continuously while the penetration depth λ increases from $\lambda(T)$, the value at zero field, to infinity [23]. The coefficient ρ has the approximate expression

$$\rho \approx \sqrt{24} \frac{\lambda}{d} \left(1 + \frac{9d^2}{\pi^6 \xi^2} \right), \quad (3.15)$$

where the second term inside the brackets accounts for surface nucleation.

If the film is part of a cavity, the variation of energy at the transition is the sum of the condensation energy and the Casimir energy, so that the previous equation becomes

$$\frac{V}{2\mu_0} \left(\frac{B_{c\parallel}^{\text{cav}}(T)}{\rho} \right)^2 = \mathcal{E}_{\text{cond}}(T) + \Delta E_{\text{cas}}(T). \quad (3.16)$$

This equation shows that it is possible to measure the contribution of Casimir energy to the total free energy variation: it consists in measuring the critical magnetic field for a stand-alone film and comparing it with a film that is part of a Casimir cavity. The relative shift is

$$\frac{\delta B_{c\parallel}}{B_{c\parallel}} \approx \frac{\Delta E_{\text{cas}}}{2\mathcal{E}_{\text{cond}}(T)}. \quad (3.17)$$

For a suitable choice of the parameters, like superconductor, metal, and dielectric materials, thicknesses, temperatures, it is possible to show experimentally that the Casimir effect enhances the critical field. The measurement has indeed been performed and shown to be fully compatible with the expectations [24].

The use of type-I superconductors for measuring the vacuum energy at the transition is thus meaningful and relies upon firm ground. Nevertheless, since the type-I superconductors are good conductors also in the normal state, the modulation of Casimir energy, with respect to total Casimir energy, $\eta = \frac{\Delta E_{\text{cas}}}{E_{\text{cas}}}$, is quite small, of order $\eta \approx 10^{-8}$ for a few nanometers thicknesses and temperatures of order 1 K [22]. With this tiny modulation it is possible to measure the effect on the critical field and on the variation of transition energy, because also the condensation energy, in type-I superconductors, is small. But it is not

sufficient to prove the weight of the vacuum, because it is in absolute too small. It is therefore necessary to consider high- T_c superconductors.

Some of their properties are of particular interest: generally high- T_c superconductors, particularly cuprates, are by construction multilayered cavities, being composed by Cu-O planes, that perform the superconducting transition, separated by nonconducting planes. More important, in a normal state, also the Cu-O planes are poor conductors, so that the variation of Casimir energy is high at the transition.

In these systems the evaluation of Casimir energy is not yet completely exploited. A first important step has been the recent analysis on the Casimir energy of a cavity composed by two flat plasma sheets at zero temperature [19,25]. The theoretical foundation is the same as for dielectric materials and conductors described above, and it is based on the summation over zero-point energies of electric modes. The approximations of the plasma sheet, with no internal dissipation, and zero temperature give to the result the status of a work that can be used as providing the order of magnitude of the effect. The calculation of the renormalized energy E_{cas} brings thus to the usual formula for two planes separated by a distance a

$$E_{\text{cas}} = -\frac{\hbar c}{2} \int \frac{d\mathbf{k}_{\perp}}{(2\pi)^2} \int_{k_0}^{\infty} \frac{dk}{\pi} \frac{k}{\omega(\mathbf{k}_{\perp}, ik)} \log t(ik), \quad (3.18)$$

where the lower integration boundary $k_0 = \mathbf{k}_{\perp}$ and the transmission coefficients t , for plasma sheets, for the TE and TM modes are given by [19]

$$(t(ik))^{-1} = 1 - \left(\frac{\Omega}{k + \Omega} \right)^2 e^{-2ka}, \quad (\text{TE}), \quad (3.19)$$

and

$$(t(ik))^{-1} = 1 - \left(\frac{\Omega k}{\mathbf{k}_{\perp}^2 - k^2 - \Omega k} \right)^2 e^{-2ka}, \quad (\text{TM}). \quad (3.20)$$

The parameter Ω is proportional to the density of the carrier in the plasma sheet [19,25],

$$\Omega \equiv \frac{nq^2}{2mc^2\epsilon_0}, \quad (3.21)$$

where n is the surface density of delocalized particles, q their electric charge, and m their mass. For small separation a the above integrals lead to the expression for energy

$$E_c(a) = -5 \times 10^{-3} \hbar \frac{cA}{a^{5/2}} \sqrt{\Omega}. \quad (3.22)$$

An estimate of the parameter Ω has been proposed recently by [26] with the aim of evaluating the Casimir effects in

high- T_c cuprates. The particles' density is estimated as $n = 10^{14} \text{ cm}^{-2}$, the charge $q = 2e$, and the mass $m = 2\alpha m_e$ with $\alpha = 5$. Inserting these values in Eq. (3.22), the reduction factor of Casimir energy with respect to the ideal case, at typical separation $a \approx 1 \text{ nm}$ turns out to be $\eta(a) = 4 \times 10^{-4} \times \sqrt{\frac{a}{1 \text{ nm}}}$. Considering that in the normal state the layer is very poorly conductive, this factor is (almost) equal to the variation of Casimir energy in the transition. Thus, the use of high- T_c superconductors leads to the gain of about 4 orders of magnitude in the modulation of Casimir energy.

The other key point is the ratio between the variation in Casimir energy at the transition and the total energy variation. In his paper [26], Kempf, checking his hypothesis with a calculation of the critical temperature T_c , has conjectured that in cuprates the whole energy variation at the transition could be due to Casimir energy. A check of this hypothesis can be done by comparing the estimated variation of Casimir energy with the total variation of the energy of the superconductor at the transition. As reported in Appendix B, in type-II superconductors the energy variation is determined by the thermodynamical critical field $B_c(T)$. In cuprates the critical field is of the order of 1 T (for a detailed description and calculation see Appendix B). The energy density variation ΔU is about

$$\Delta U \approx \frac{B_c^2}{2\mu_0} \approx 4 \times 10^5 \text{ J/m}^3. \quad (3.23)$$

The variation of Casimir energy density ΔU_{cas} is, following the Kempf estimate,

$$\Delta U_{\text{cas}} \approx \eta(a) \frac{N\pi^2 \hbar c}{720 a^3} \approx 2 \times 10^5 \text{ J/m}^3, \quad (3.24)$$

where $N \approx 10^9$ is the number of cavities per unit height. The two energies are indeed, roughly, of the same order of magnitude.

Notice that, as stated in Ref. [26], the separation among the plates being of order of 1 nm, the ‘‘Casimir’’ energy is dominated by plasmons (i.e., by the Van der Waals) energy with respect to vacuum energy. Thus, our assumption of Kempf’s hypothesis should be regarded also as a starting point for further investigations on high- T_c superconductors, to be performed in the near future, directed in two ways. First, regarding the present analysis as an order of magnitude estimate, evaluate more accurately the Casimir energy variation at the transition and its contribution to total energy; second, extend it to superconductors with higher spacing among conducting planes until the conditions already studied in previous measurements with metallic plates [21,22,24] are recovered.

The actual modulation of the effect can be performed in two ways: (1) By applying a time dependent magnetic field that spoils the superconducting state so as to have zero

magnetization in both initial and final states; in this condition the actual measurement can be performed in a nonvanishing applied field, because the magnetization is brought to zero and the interaction with the magnetic field is minimized also at the final state. (A further possibility is to put the sample in two different conditions of superconductivity, with more or fewer regions where the sample is superconducting, both at a vanishing applied field: this can be obtained by using hysteretic superconductors. Among them, as an example, are the cuprates.) (2) By temperature modulation in a vanishing field. Both cases have no latent heat (see also Appendix B).

The quantity that will generate the variation of gravitational force on the sample is (the variation of) the internal energy UV , where V is the volume of the sample of the superconductor. The variation of internal energy density U is evaluated for the two modulation cases in Appendix B. It is given by the equation (see (B13))

$$\Delta U = \int_T^{T_c} C_n dT + \frac{B_0^2}{2\mu_0} [1 - (T/T_c)^2]^2 + 2 \left(\frac{T}{T_c} \right)^2 [1 - (T/T_c)^2]. \quad (3.25)$$

This is the sum of three terms: the internal energy variation of the normal state (present only in the case of temperature modulation), the contribution of the Gibbs energy, and the contribution of entropy. The third term, for temperatures near T_c , gives the biggest contribution. This equation shows that the variation of internal energy is proportional to and roughly of the same order of magnitude of the energy of the thermodynamical critical field and, under the Kempf estimate, it is expected to be of the same order of magnitude of Casimir energy variation. Thus, as stated before, we assume the Kempf hypothesis and estimate the energy variation as totally due to the Casimir effect. It is very important to stress that, as will be shown in Secs. III and IV, even if the contribution of Casimir energy were of order of just a few over a thousand of the total energy at the transition, we might ascertain whether it gravitates.

In the following sections the detection of small forces by using the best of current optical techniques will be considered. The use of high- T_c superconductors in high sensitivity optical devices is a field yet to be investigated, in particular in macroscopic devices. Nevertheless, present superconductors can be deposited on quite large surface optical elements: YBCO is well deposited on aluminum (Al_2O_3) substrates, which are the best substrates also for optics at low temperature. Indeed, a 300 nm thick YBCO layer deposited on a 3 in. diameter, 5 mm thick Al_2O_3 substrate produced by CERACO is presently under test in our laboratory. Notice that, even if the first test will be performed with YBCO for its robustness, the use of low upper critical field superconductors should be preferred, since they allow simpler magnetic modulation at equal

values of the thermodynamical critical field (see also Appendix B for definitions of thermodynamical and upper critical field). Furthermore, much larger thicknesses can be reached by using superconducting crystals.

IV. USE OF GRAVITATIONAL WAVE DETECTORS

The force exerted by the gravitational field when the Casimir energy contained in the superconductor system is modulated should be compared with the up-to-date technology in the detection of small forces in macroscopic systems. Two main ways might be followed. The first way is to make use of the present most sensitive apparatuses in the detection of small forces, the gravitational wave detectors; the second is to go towards lower frequencies and use torsion pendulums. In the following we will consider first the use of gravitational wave detectors. The main reason to explore this way is the possibility of making use of a very well developed technology in force detection and seismic attenuation. Another not negligible reason is that money can be saved if a replica of many instruments and methods already available is avoided. In this case, it is necessary to recover an experimental method, discussed later, to apply a force on such detectors (only at a given frequency) without perturbing the gravitational wave measurement in the other frequencies of the spectrum. Our comparison can start with the present state of the art of gravitational wave detectors. Over the past decades, this field has known many impressive technical improvements and developments. The two most sensitive detectors of gravitational waves, LIGO and Virgo, have demonstrated the feasibility of all foreseen techniques, by reaching, and in some frequency regions superseding, the sensitivities expected for the first generation detectors [27,28]. Moreover, many important techniques already compliant or extremely useful in the next generation detectors have been demonstrated worldwide, i.e., in LIGO [29], in Virgo [30], or in the medium-scale detectors like GEO [31] or still in development like Kagra [32]. In light of all this progress it is very reasonable to expect, for the second generation of such detectors, the so-called advanced detectors, presently under construction, to reach the design sensitivities in the next few years [33,34].

In this case the frequency region of highest sensitivity \tilde{S}_F to the force lies in the range from 20 to 40 Hz; if a gravitational wave test mass of 42 kg is considered, the value, in this region, is of order of $\tilde{S}_F \approx 10^{-13} \text{N}/\sqrt{\text{Hz}}$.

Glancing at future detectors, the so-called third-generation detectors, like the Einstein Telescope (ET), we see that they will benefit of low seismic sites, low temperature, and suitably injected power for low-frequency detection. The expected sensitivity in the amplitude of the force will gain about 2 orders of magnitude, showing the region of best force sensitivity at frequencies slightly smaller than 10 Hz [35].

Two main conditions, in our opinion, constrain and define the use of gravitational wave detectors also for a measurement of the weight of vacuum. The first is that no modifications are allowed to the gravitational wave detector that in any case risk to reduce the gravitational wave sensitivity. In particular, no changes of the suspensions chain, of the payloads, of the actuators will be allowed: the system providing the force should be “external” and sufficiently far from the gravitational wave test masses so as to avoid introducing spurious signals. The second is that the vacuum weight force is vertical (i.e., orthogonal to the Earth’s surface) while the gravitational detectors are designed to detect horizontal forces (i.e., almost parallel to the Earth’s surface, with a small coupling factor with the vertical due to Earth’s curvature and mechanical imperfections).

A possible way to face both points is to build an *ad hoc* apparatus, lying several meters from the gravitational wave detectors test masses; let us call it the Archimedes system. In this system, a mass, over which the superconducting material is deposited, is suspended and is free to move vertically for frequencies above a few Hz. By applying the modulation technique discussed previously, a force is exerted on the mass. To transport this force from the mass of the Archimedes system to the test mass of the gravitational wave detector, the ideal way would be to link them with a spring. It is not possible, for the reasons discussed above, to use a mechanical spring but, as we shall see, it is possible to link the two masses via the radiation pressure, by realizing an optical cavity that, in a properly detuned configuration, acts as an optical spring [36].

To show the behavior of an optical spring, let us consider a Fabry-Perot cavity with a suspended perfectly reflective end mirror and a fixed highly reflective input mirror, and analyze it in the static approximation, valid for frequencies lower than cavity linewidth. Suppose that it is illuminated by a laser light with frequency ω_0 and power I_0 . Assuming the cavity to be close to resonance, we list several quantities characterizing the state of the cavity, i.e., its linewidth γ , finesse F , circulating power W , and phase shift Φ gained by the light as it comes out from the cavity, in terms of more basic parameters,

$$\gamma = \frac{cT_I}{4L}, \quad (4.1)$$

$$F = \frac{2\pi}{T_I}, \quad (4.2)$$

$$W(I_0, \delta_\gamma) = \frac{4I_0}{T_I} \frac{1}{(1 + \delta_\gamma^2)}, \quad (4.3)$$

$$\Phi(\delta_\gamma) = -2\tan^{-1}(\delta_\gamma). \quad (4.4)$$

Here L is the cavity length and T_I the input-mirror power transmissivity. The detuning parameter δ_γ ,

$$\delta_\gamma \equiv \frac{\delta}{\gamma}, \quad (4.5)$$

is defined in terms of $\delta \equiv \omega_{\text{res}} - \omega_0$, the difference between the cavity resonant frequency and laser frequency. The ponderomotive force F_p , the radiation pressure, is given by

$$F_p = \frac{2W}{c}. \quad (4.6)$$

If the suspended mirror moves by an amount δx , since the cavity is not perfectly on resonance, the amount of light inside the cavity changes, and hence the radiation pressure on the mirror: a restoring force F_r is produced equal to $F_r = -K_{\text{opt}}\delta x$, where K_{opt} is the optical spring constant, given by

$$K_{\text{opt}} = \frac{2}{c} \frac{\partial W(I_0, \delta_\gamma)}{\partial \delta_\gamma} \frac{\partial \delta_\gamma}{\partial x} = -\frac{4\omega_0 W}{\gamma L c} \frac{\delta_\gamma}{(1 + \delta_\gamma^2)}. \quad (4.7)$$

With some algebra it can be written as

$$K_{\text{opt}} = -\frac{4\omega_0 I_0 \delta_\gamma}{c^2} \left[\frac{2F}{\pi} \frac{1}{(1 + \delta_\gamma^2)} \right]^2. \quad (4.8)$$

The optical spring constant can be positive or negative, depending on the sign of the detuning δ_γ . We choose a negative detuning so that the constant is positive. Remarkably, the optical spring constant, for sufficiently high finesse, can be quite high. For example, suppose we have a cavity with finesse $F = 6 \times 10^5$, input power $I_0 = 0.16$ mW, detuning $\delta_\gamma = -0.3$, and laser frequency $\omega_0 = 3 \times 10^{14}$ Hz (corresponding to laser yttrium aluminum garnet wavelength of $1.064 \mu\text{m}$); the optical spring constant is then equal to $K = 7.8 \times 10^4$ N/m. If the cavity is composed by two or more suspended mirrors, a similar analysis applies and the light acts as a spring. The other key feature of the optical spring is the low noise reintroduced: if we assume that the laser is shot noise limited, the fluctuation power incident on the cavity is $\tilde{I}_0 = \sqrt{2\hbar\omega_0 I_0}$, and this induces a fluctuating noise force

$$\begin{aligned} \tilde{F}_n &= \frac{2}{c} \frac{\partial W(I_0, \delta_\gamma)}{\partial I_0} \tilde{I}_0 = \left(\frac{2F}{\pi} \frac{1}{(1 + \delta_\gamma^2)} \right) \frac{2\sqrt{2\hbar\omega_0 I_0}}{c} \\ &= 6 \times 10^{-15} \frac{\text{N}}{\sqrt{\text{Hz}}}. \end{aligned} \quad (4.9)$$

This small value of injected noise arises from the small amount of light that circulates in the cavity, even in the presence of a high spring constant, a condition that can be reached by using high finesse cavities. The actual apparatus is sketched in Fig. 2: the cavity is composed by 5 optical elements. An input mirror is coated with superconducting material, except for a small area to let the light pass. This mirror has the surface parallel to the ground. A 45°

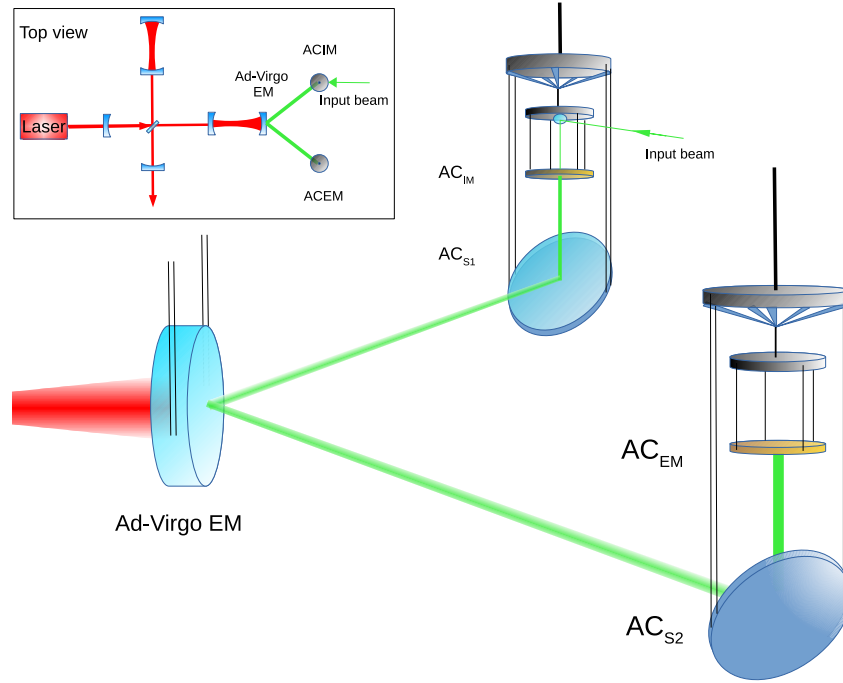


FIG. 2 (color online). The optical link. The cavity acting as an optical spring is composed by the Archimedes cavity input mirror, AC_{IM} , by the steering mirror AC_{S1} , by the back surface of the gravitational wave detector test mass, Ad-Virgo EM, by a second steering mirror AC_{IM} and closed by the Archimedes cavity end mirror AC_{EM} . Also a top view of the apparatus and the gravitational wave detectors is sketched in the top-left box, not to scale, to show a complete view. The cavity is illuminated by a laser reflecting on the upper stage that suspends the input mirror, as shown.

reflective mirror lying below the input mirror sends the beam to the back surface of the gravitational wave detector test mass. The beam impinges upon the mirror at a few degrees in the horizontal plane; hence it is reflected towards a second Archimedes apparatus that closes the cavity. The mirrors of the Archimedes apparatuses coated with the superconductor have masses $m = 5$ kg and are suspended to a seismic isolation system similar to Virgo ones. The 45° mirrors are suspended to the same attenuation system, but at an upper stage, to be independent of the mirrors coated with the superconductor: they act merely as deflection mirrors. They are quite heavy, of the same order of magnitude of the gravitational wave test mass. The superconductor covers on the two faces of each coated mirror an area $S = 0.23$ m², on each mirror, with a thickness of about 250 μ m. The substrate is Al₂O₃, which is particularly well suited to low temperature work. The area is similar to the present beam splitter of the Virgo detector.

The amplitude of force modulation F_m can be evaluated as

$$F_m \approx N\eta(a) \frac{E_{(Cp)}}{c^2} g \approx \mathcal{N} \left[-5 \times 10^{-3} \hbar \frac{cA}{a^{5/2}} \sqrt{\Omega} \right] \approx 10^{-15} N, \quad (4.10)$$

where η is the reduction factor with respect to the perfectly reflecting plates Casimir energy $E_{(Cp)}$ [26], $\mathcal{N} = 1.6 \times 10^5$ is the total number of layers, and $a = 1.17$ nm is the conducting layers separation in YBCO. To compare the effect of this force

with the sensitivity of the gravitational wave detector, we will compare the displacement induced in the gravitational test mass with respect to the displacement sensitivity. Note that, if the gravitational wave detector test mass is linked by an optical spring to other free masses, under the condition presently assumed of small distances, with respect to arm length (and not considering the region of frequency around the optical spring resonance frequency), the displacement of the gravitational wave test mass induced by a gravitational wave will not change because all masses will accelerate at once. Note that this statement also assumes that the masses of the gravitational wave detector are free. This is not strictly the case: the mass is linked by the arm-cavity optical spring to the rest of the masses of the gravitational wave interferometer. To reach a precise statement, and not an order of magnitude expectation, a complete simulation of the Archimedes cavity coupled to the interferometer should be performed, which because of the complexity, is outside the aim of the present paper and will be investigated in the near future. At present, a complete simulation of the Archimedes cavity has been performed. The system has been simulated by using the OPTICKLE code [37]. Under the assumptions and the parameters discussed above, the expected signal for an integration time of 6 months, a typical time scale of a run, is given in Fig. 3.

The signal is above the sensitivity by 2 orders of magnitude at low frequency, while it falls under the Advanced Virgo sensitivity around 100 Hz. As expected,

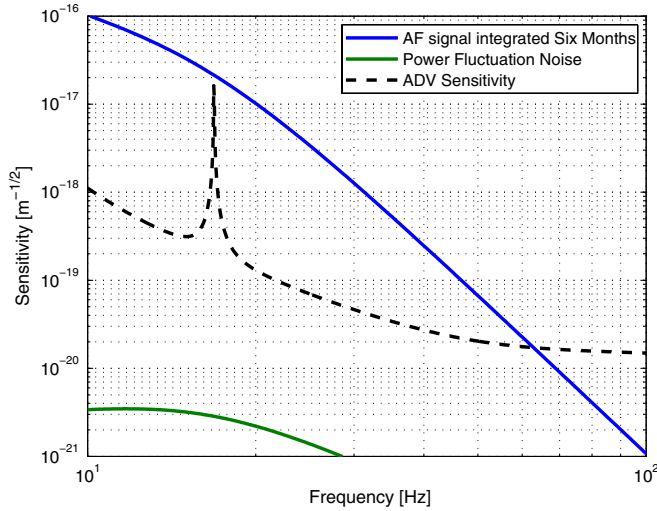


FIG. 3 (color online). Expected signal for the YBCO actuator described in the previous section.

the noise due to power fluctuations is negligible. Indeed, the power inside the cavity is about 60 W, to be compared with the 0.6 MW of light circulating in the gravitational wave arm cavity. In conclusion, the use of the optical spring to transport the force from the actuator system to the gravitational wave mass makes it possible to locate the actuator several meters away from the gravitational wave detector mass, avoiding possible spurious interactions. The suspension system of the Archimedes force apparatus can be a replica of the ones of gravitational wave detectors, and the cryogenic system can benefit from the several experimental studies and realizations now making progress in the world [32]. In this way, the optical system reduces to the optical spring actuator, which is relatively simple, being just a laser suitably locked on the cavity.

Note that, if the same system were applied to the next generation of gravitational wave detectors, in particular Einstein Telescope low-frequency [35,38], a remarkable improvement is expected. This is shown in Fig. 4. The cavity considered to perform the optical spring is similar to the previous one, with masses of 10 kg and a larger finesse = 1.5×10^6 , that is not far from the current technological achievements. The input power is $P_{in} = 1.6 \times 10^{-4}$ (not critical). The input power noise has been taken as the shot-noise limit of the input power, equivalent to the noise-to-power ratio of about $5 \times 10^{-8} 1/\sqrt{\text{Hz}}$: the power noise is more critical in this case but is negligible, remaining an order of magnitude lower than the sensitivity. Figure 4 shows that with an integration time of 6 months, the signal-to-noise ratio of about $S/R = 10^4$ is reached. This means that a signal-to-noise ratio of 1000 might be reached in a couple of days.

With such high signal-to-noise ratios, measurements with different materials and different layer separations up to tens of nanometers would then be possible, allowing a complete campaign of studies. This possibility clarifies also our

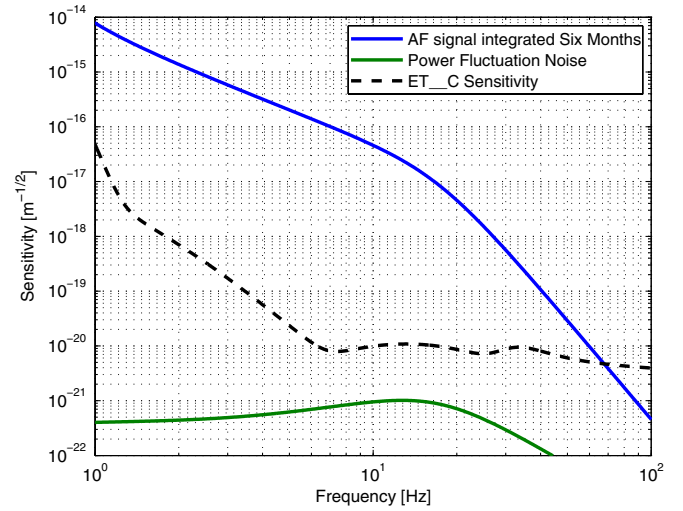


FIG. 4 (color online). Expected signal when using ET optimized for low frequency.

working case on the Kempf hypothesis. According to that recipe, all the condensation energy, at both small and larger layer separations, results from Casimir energy. With this sensitivity, considering the accuracy of the gravitational wave detectors, even if the contribution of Casimir energy were only a few parts over a thousand, we might test whether it gravitates.

V. USE OF BALANCES

The use of balances might be favored by the possibility to go towards low frequencies. Indeed, the modulation of superconducting phase transitions in macroscopic bodies is expected to be easier at lower frequencies. Furthermore, we will consider here the possibility of performing force modulation also by temperature modulation. We evaluate the thermal noise at the temperature working point of 100 K, near the YBCO transition temperature. The main experimental point that has to be faced in going towards low frequencies is that a proper seismic attenuation system for balances does not yet exist.

A possible way to reduce seismic noise at frequencies lower than 0.1 Hz is to hang the balance to a cascade formed by an inverted pendulum followed by a blade's isolation stage, as shown in Fig. 5. The inverted pendulum is efficient in the two horizontal translational degrees of freedom and the rotation around the vertical axis, while the blades' stage is efficient in the vertical degree of freedom and in the rotations [30,39]. The Virgo inverted pendulum has already been demonstrated to have a resonant frequency of 0.03 mHz, and work is ongoing to further reduce it to the value of 0.01 Hz. Also the blades' stage resonance can be tuned, by careful tuning of magnetic antispring stiffness, to similar values.

The control of this top stage can be done either at a very low frequency, with a unity gain of the feedback lower than the resonance, or in high bandwidth, with a unity gain of about 1 Hz. Here we assume to close the loop in

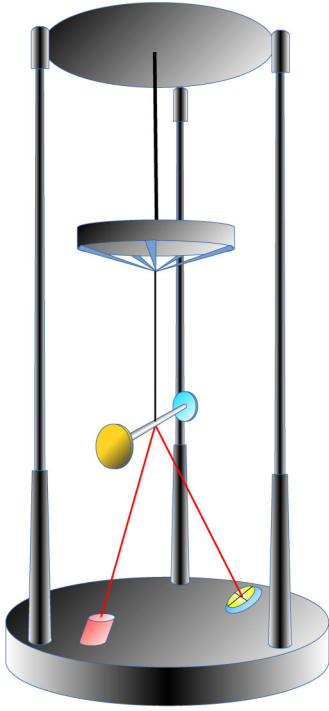


FIG. 5 (color online). The balance with the optical lever detection readout. The seismic attenuation chain is composed by the three-legs inverted pendulum and by the blades-attenuation element. The readout is composed by a laser beam that reflects on the bottom of the bar and impinges on a quadrant photodiode.

high gain and reach, at the suspension point of the balance, the electronic noise floor of the accelerometers $a_s \approx 4 \times 10^{-10} \text{ m}^2/\text{s}\sqrt{(\text{Hz})}$, corresponding to the displacement noise of $1 \text{ nm}/\sqrt{(\text{Hz})}$ at 0.1 Hz, and flat for a frequency less than 0.1 Hz [39]. To calculate the expected signal and noises at the balance, we have considered a balance having arms of length $L = 0.1 \text{ m}$, a plate at each arm's end of mass $M = 0.4 \text{ kg}$, a total mass $M_b = 1.25 \text{ kg}$, a moment of inertia $I = 0.01 \text{ kg m}^2$, and a resonance frequency $F_{\text{res}} = \omega_b/2\pi = 5 \text{ mHz}$, with mechanical internal loss angle $\phi = 10^{-6}$. The resonance value is higher than the typical torsion pendulum (horizontal) ones already existing [40] and takes into account the feasibility of a real vertical balance: in particular, the resonance of 5 mHz corresponds to a careful setting of the bending point distance from the balance center of mass of about $h_b \approx 1 \mu\text{m}$. (The bending point is the physical point around which the balance rotates. Its position depends upon the point where the wire is fixed on the balance, the mass of the balance, and the wire section and Young's modulus. The distance h_b of the bending point from the balance center of mass determines the balance's resonance frequency ω_b , with the relation $\omega_b^2 = \frac{M_b g h_b}{I}$. This distance can be tuned mechanically, by regulating the ballasts' position, and in feedback, with the help of external forces.)

The material to be used for the suspension fiber (and for the balance itself) cannot be fused silica, which is the

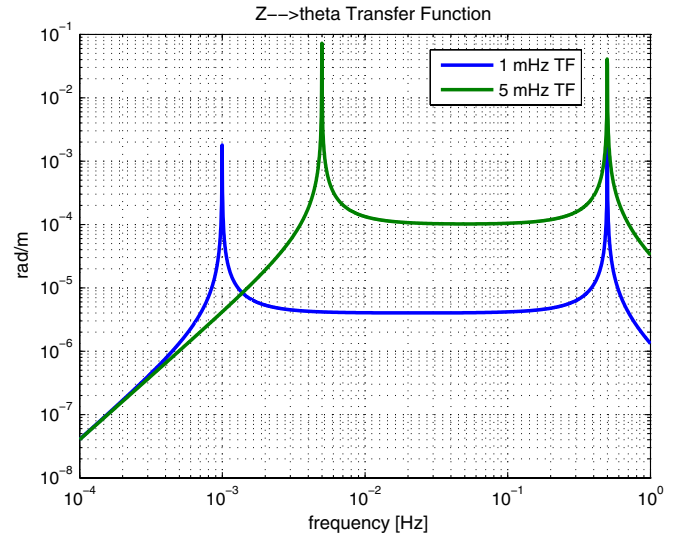


FIG. 6 (color online). Transfer function from the displacement suspension point to the balance's tilt for 1 mHz and 5 mHz resonance frequency. The coupling depends on the resonant frequency.

material of choice for the test masses of all first-generation gravitational wave detectors, because it has a high dissipation at low temperatures [41,42]. Sapphire has already been proposed as an alternative material also for the suspension fiber, and here we assume it is the final material [43]. The wire length considered in our simulation is of 1 m and the diameter $d = 50 \mu\text{m}$. The end plates have radius $R = 0.15 \text{ m}$, made by a sapphire substrate, and one is coated with $250 \mu\text{m}$ of YBCO on both faces: the force modulation on the plate is $F_a = 4 \times 10^{-16} \text{ N}$. As expected, simulations show that the most critical noise is the seismic noise injected through the coupling of the transversal motion of the suspension point to the tilt of the balance. The simulated transfer function is shown in Fig. 6 for the case of 5 mHz and for a very optimistic case, similar to torsion pendulum value, of 1 mHz to show that this parameter is critical for reaching a significant attenuation.

The tilt signal can in principle be read off in various ways. A high-sensitivity possibility is to use a second balance and read the ends' differential displacements with a Michelson interferometer having a Fabry-Perot cavity at the ends of the balances' arms. For an interferometer having arm cavity finesse $F_b = 100$, input power $P_b = 0.01 \text{ W}$, the sensitivity is reported in Fig. 7 where the radiation pressure noise and shot noise are plotted. The signal (blue curve) is obtained by integrating for 6 months and is approximately 2 orders of magnitude larger than the total noise (black curve).

Under the assumption on seismic noise reduction the sensitivity is limited at low frequency by suspension thermal noise and by seismic noise for frequencies larger than 30 mHz. The radiation pressure noise and shot noise curves ensure that fundamental noises will not make it impossible to perform the measurement of the vacuum-gravity force.

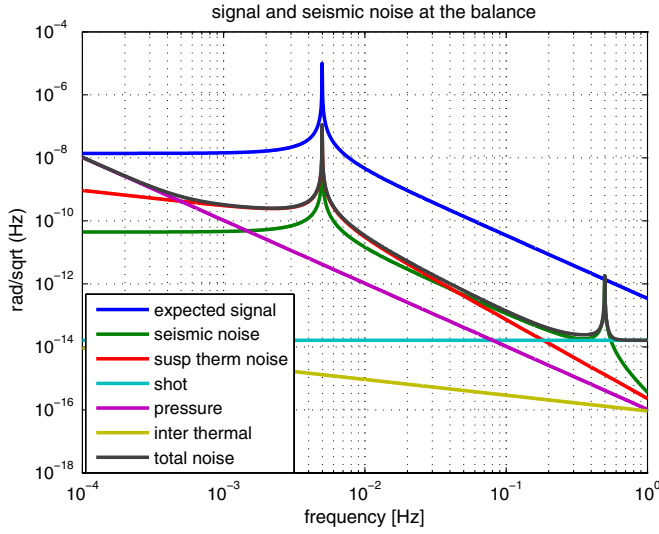


FIG. 7 (color online). Expected signal and noises for the balance. In the region of frequencies $5 < f < 100$ mHz the signal is about 2 orders of magnitude above the noise.

Nevertheless, the noise is so low with respect to other noises that other tilt detection methods, even if noisier, can be exploited if simpler. As an example, optical lever systems or capacitors used in torsion pendulums have already shown remarkable sensitivities; they are not yet fully compatible with our needs, but surely deserve careful study and attention [40,44]. The use of such a detection system is also sketched in Fig. 5: a low power laser beam is sent to the balance and reflected towards a quadrant photodiode; a tilt of the balance displaces the impinging point of the beam on the photodiode, and a signal is hence generated.

The corresponding signal and noises in $N/\sqrt{\text{Hz}}$ are plotted in Fig. 8. The coupling of suspension point acceleration a_s can be interpreted as producing a moment of inertia $M_s = M_b \cdot a_s \cdot h_b$, equivalent to the noise force

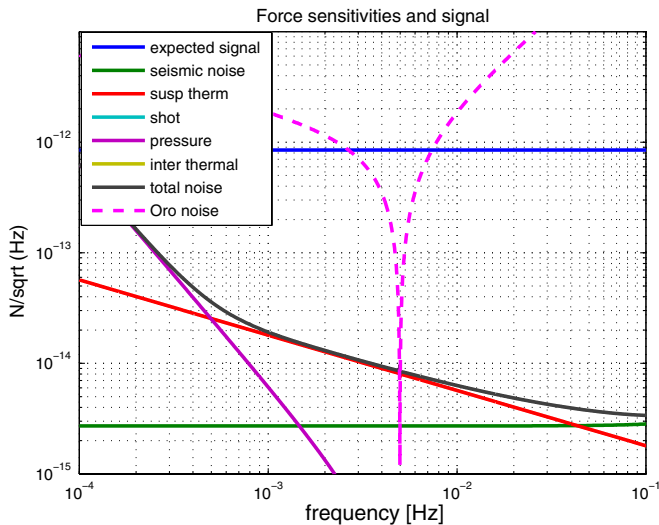


FIG. 8 (color online). Force signal and noises. The dashed line describes the noise of an optical lever detection system.

$M_b \cdot a_s \cdot h_b / L_b$, that again shows how the setting of the bending point is critical. The plot reports (dashed line) also the readout noise of an optical lever demonstrated in Ref. [44]: such a system makes it mandatory to perform the measurement in the neighborhood of the resonance (at the price of slightly reducing the sensitivity), but leads to a remarkable simplification of the detection method.

VI. CONCLUSIONS

We have shown that it is by now possible to begin the experimental path to check against observation whether virtual photons do gravitate and to verify the Archimedes force of vacuum. Various experimental techniques must be investigated and refined, i.e., deposition of thick layers of high- T_c superconductors in optical substrates, application of optical springs to connect different apparatuses, and improvements in low-frequency seismic isolation. If these improvements, not far from the present technological achievements, will be successful, a first answer will be given to one of the deepest and long-lasting problems of fundamental physics.

ACKNOWLEDGMENTS

L. D. F. and G. E. are grateful to Dipartimento di Fisica of Federico II University for hospitality and support. Previous collaboration with G. Bimonte on several theoretical aspects has been of great importance. We are grateful to M. Cerdonio, A. Coltorti, F. Fidecaro, F. Frasconi, E. Majorana, P. Rapagnani, and F. Ricci for useful discussions.

APPENDIX A: DIELECTRIC CONDUCTIVITY IN TYPE-I SUPERCONDUCTORS

In the case of a Bardeen-Cooper-Schrieffer conductor at a temperature $T < T_c$, the expression of $\sigma'_s(\omega)$ can be written as

$$\sigma'_s(\omega) = \kappa\delta(\omega) + \tilde{\sigma}'_s(\omega). \quad (\text{A1})$$

For $\omega > 0$, $\tilde{\sigma}'_s(\omega)$ reads as [45]

$$\tilde{\sigma}'_s(\omega) = \frac{\hbar n e^2}{2m\omega\tau_n} \left[\int_{\Delta}^{\infty} dE J_T + \theta(\hbar\omega - 2\Delta) \int_{\Delta-\hbar\omega}^{-\Delta} dE J_D \right], \quad (\text{A2})$$

where

$$J_T := g(\omega, \tau_n, E) \left[\tanh \frac{E + \hbar\omega}{2KT} - \tanh \frac{E}{2KT} \right], \quad (\text{A3})$$

$$J_D := -g(\omega, \tau_n, E) \tanh \left(\frac{E}{2KT} \right), \quad (\text{A4})$$

with K the Boltzmann constant. Defining

$$P_1 := \sqrt{(E + \hbar\omega)^2 - \Delta^2}, \quad P_2 := \sqrt{E^2 - \Delta^2}, \quad (\text{A5})$$

the function $g(\omega, \tau_n, E)$ is

$$g := \left[1 + \frac{E(E + \hbar\omega) + \Delta^2}{P_1 P_2} \right] \frac{1}{(P_1 - P_2)^2 + (\hbar/\tau_n)^2} - \left[1 - \frac{E(E + \hbar\omega) + \Delta^2}{P_1 P_2} \right] \frac{1}{(P_1 - P_2)^2 + (\hbar/\tau_n)^2}.$$

$$\kappa = \frac{\pi n e^2}{m} \left[\frac{\pi \tau_n \Delta}{\hbar} \tanh \frac{\Delta}{2KT} - 4\Delta^2 \int_{\Delta}^{\infty} dE \frac{\tanh(E/2KT)}{\sqrt{E^2 - \Delta^2} [4(E^2 - \Delta^2) + (\hbar/\tau_n)^2]} \right]. \quad (\text{A7})$$

APPENDIX B: INTERNAL ENERGY VARIATION IN TYPE-II SUPERCONDUCTORS' TRANSITIONS

Measuring the variation of weight of the superconductor when it undergoes a transition means to measure the variation of its internal energy among the two states, normal and superconducting. The internal energy difference of the system in different states can be evaluated by means of the thermodynamical potentials H' (enthalpy), G (Gibbs free energy), and S (entropy).

For a magnetic material the differential of the internal energy dU may be written in terms of the temperature T , the applied magnetic field \mathbf{B} , and the magnetization \mathbf{M} of the material as

$$dU = TdS + \mathbf{B} \cdot d\mathbf{M}. \quad (\text{B1})$$

The enthalpy is defined as

$$H' \equiv U - \mathbf{B} \cdot \mathbf{M}, \quad (\text{B2})$$

and finally the Gibbs free energy as

$$G \equiv H' - TS, \quad (\text{B3})$$

with differential form

$$dG = -SdT - \mathbf{M} \cdot d\mathbf{B}. \quad (\text{B4})$$

In type-II superconductors, for applied field $\mathbf{B}(T)$, where T is the temperature, they are defined as the lower critical field, such that if $B \leq B_{c1}(T)$ the field does not penetrate in the sample, and the upper critical field $B_{c2}(T)$ such that if $B \geq B_{c2}(T)$, the superconductivity is destroyed. In analogy with type-I superconductors, a thermodynamical critical field $\mathbf{B}_c(T)$ is defined such that the difference of Gibbs free energies, at given temperature, among the superconducting and normal states at zero applied field is

The coefficient κ of the Dirac delta in Eq. (A1) is determined so as to satisfy the sum rule

$$\int_0^{\infty} d\omega \sigma'(\omega) = \frac{\pi n e^2}{2m}, \quad (\text{A6})$$

where $n = n_s + n_n$ is the total electron density and can be computed exactly according to [45]

$$G_s(T, 0) - G_n(T, 0) = \frac{(B_c(T))^2}{2\mu_0}. \quad (\text{B5})$$

Following the Ginzburg-Landau theory the lower critical field B_{c1} and the upper critical field B_{c2} are linked to the thermodynamical critical field B_c by the dimensionless parameter $k = \frac{\lambda(T)}{\xi(T)}$,

$$B_{c1} = \frac{B_c \log k}{\sqrt{2}k}, \quad (\text{B6})$$

and

$$B_{c2} = B_c \sqrt{2}k. \quad (\text{B7})$$

The temperature dependence of the critical field $B_c(T)$ is well approximated by

$$B_c(T) = B_c(0) \left[1 - \left(\frac{T}{T_c} \right)^2 \right], \quad (\text{B8})$$

and similarly for $B_{c1}(T)$ and $B_{c2}(T)$.

In high- T_c superconductors like YBCO, k is of order of 100. The entropy of the superconductor in the applied field, to take heuristically into account the magnetization of the superconductor and fit experimental data [46], is approximated as

$$S_s(T, B) = S_n(T) + \chi'(T) \frac{(B_{c2}(T) - B)}{\mu_0} \frac{dB_{c2}}{dT}, \quad (\text{B9})$$

where $\chi'(T) = \mu_0 \frac{\partial M}{\partial B}$ is called the differential susceptibility. It takes into account the anisotropy of type-II superconductors and maintains the entropy at the vanishing field independent of the anisotropic value of B_{c2} . This expression for the entropy shows that in type-II superconductors, unlike the type-I case, the transition obtained by applying an external field at fixed temperature $T \leq T_c$ is of second order, with no latent heat. The transition in the vanishing

field for $T = T_c$ is of second order, since $B_{c2}(T_c) = 0$. Thus, both modulation techniques proposed show an absence of latent heat. Let us observe that, if the applied field $B \leq B_{c1}(T)$ and the transition is obtained by increasing the temperature T , the superconductor behaves like a type-I superconductor (the field does not penetrate and there is an entropy variation). The transition is thus of first order, with latent heat Lh equal to

$$Lh = T_c(B)(S_n - S_s) = \frac{B_{c1}^2}{2\mu_0} \left(\frac{T_c(B)}{T_c} \right)^2 \times \left[1 - \left(\frac{T_c(B)}{T_c} \right)^2 \right]. \quad (\text{B10})$$

As stated in Sec. II, the transitions considered in the present paper are two: the first is a transition by temperature

variation in the vanishing field. The second is a field variation up to $B_{c2}(T)$ at constant T . Both cases have no latent heat. To evaluate the internal energy variation ΔU , in the first case, considering the vanishing field and noticing that $G_s(T_c) = G_n(T_c)$, we can write

$$S_s(T) - S_n(T) = -\frac{dG_s(T, 0)}{dT} + \frac{dG_n(T, 0)}{dT} = \frac{1}{2\mu_0} \frac{d[B_c(T)]^2}{dT} = \frac{B_c(T)}{\mu_0} \frac{dB_c(T)}{dT}. \quad (\text{B11})$$

In the vanishing field the variation of internal energy ΔU is equal to the variation of enthalpy. By using (B3) this variation can be written as

$$\begin{aligned} \Delta U &= H'_n(T_c) - H'_s(T) = H'_n(T, 0) + \int_T^{T_c} C_n dT - H'_s(T, 0) \\ &= \int_T^{T_c} C_n dT + G_n(T) + TS_n(T) - G(T, 0) - TS_s(T, 0) \\ &= \int_T^{T_c} C_n dT + \frac{B_c(T)^2}{2\mu_0} - T \frac{B_c(T)}{\mu_0} \frac{dB_c(T)}{dT}. \end{aligned} \quad (\text{B12})$$

Considering that $B_c(T) = B_0[1 - (T/T_c)^2]$, the variation of energy can be written as the sum of three terms: the internal energy variation of the normal state, the contribution of the Gibbs free energy, and the contribution of entropy. The third term, for temperatures near T_c , gives the biggest contribution, and one has

$$\begin{aligned} \Delta U &= \int_T^{T_c} C_n dT + \frac{B_0^2}{2\mu_0} [1 - (T/T_c)^2]^2 \\ &\quad + 2 \left(\frac{T}{T_c} \right)^2 [1 - (T/T_c)^2]. \end{aligned} \quad (\text{B13})$$

This equation shows that the variation of internal energy is proportional to, and roughly of the same order of magnitude as, the energy of the thermodynamical critical field.

The second transition is provided by keeping the temperature T fixed and by varying the applied field from zero to the critical field $B_{c2}(T)$. Notice that, being the energy scale given by the thermodynamical critical field, the use of low- k materials should be preferred, to maintain the upper critical field as manageable. Notice that in this transition the magnetization of the sample is zero both at the start and at the end of the transition; hence it is expected that the variation of internal energy due to the superconductive contribution is equal to the previous case. The normal-state contribution, on the contrary, is zero because there is no temperature variation. The above expectations can be verified by noticing that $U = G + \mathbf{B} \cdot \mathbf{M} + TS$. The differential reads

$$\begin{aligned} dU &= TdS + \mathbf{B} \cdot d\mathbf{M} = TdS + \mathbf{B} \cdot d\mathbf{M} + \mathbf{M} \cdot d\mathbf{B} - \mathbf{M} \cdot d\mathbf{B} + SdT - SdT \\ &= d(TS) + d(\mathbf{M} \cdot \mathbf{B}) + dG. \end{aligned} \quad (\text{B14})$$

By integration among the two final states we obtain

$$\Delta U = T(S_n(T) - S_s(T)) + G_n(T) - G_s(T, 0), \quad (\text{B15})$$

which gives the same result of (B13) without the contribution of the normal state.

- [1] S. Weinberg, *Rev. Mod. Phys.* **61**, 1 (1989).
- [2] C. Rovelli, *Quantum Gravity* (Cambridge University Press, Cambridge, England, 2004).
- [3] B. S. DeWitt and G. Esposito, *Int. J. Geom. Methods Mod. Phys.* **05**, 101 (2008); G. Esposito, *An Introduction to Quantum Gravity*, EOLSS Encyclopedia (UNESCO, Paris, France, 2011).
- [4] C. Kiefer, *Quantum Gravity*, International Series of Monographs on Physics Vol. 155 (Clarendon, Oxford, 2012).
- [5] E. Bianchi and C. Rovelli, *Nature (London)* **466**, 321 (2010).
- [6] T. Padmanabhan, *Int. J. Mod. Phys. D* **15**, 2029 (2006).
- [7] E. Calloni, L. Di Fiore, G. Esposito, L. Milano, and L. Rosa, *Phys. Lett. A* **297**, 328 (2002).
- [8] S. A. Fulling, K. A. Milton, P. Parashar, A. Romeo, K. V. Shajesh, and J. Wagner, *Phys. Rev. D* **76**, 025004 (2007).
- [9] G. Bimonte, E. Calloni, G. Esposito, and L. Rosa, *Phys. Rev. D* **74**, 085011 (2006); **75**, 049904(E) (2007); **75**, 089901(E) (2007); **77**, 109903(E) (2008).
- [10] K. A. Milton, S. A. Fulling, P. Parashar, A. Romeo, K. V. Shajesh, and J. A. Wagner, *J. Phys. A* **41**, 164052 (2008).
- [11] K. V. Shajesh, K. A. Milton, P. Parashar, and J. A. Wagner, *J. Phys. A* **41**, 164058 (2008).
- [12] K. A. Milton, K. V. Shajesh, S. A. Fulling, and P. Parashar, *Phys. Rev. D* **89**, 064027 (2014).
- [13] G. Bimonte, E. Calloni, G. Esposito, and L. Rosa, *Phys. Rev. D* **76**, 025008 (2007).
- [14] A. Einstein, *Jahrb. Radioakt. Elektron.* **4**, 411 (1907); **5**, 5 (1908); **5**, 98 (1908); [translated by H. M. Schwartz, *Am. J. Phys.* **45**, 512 (1977); **45**, 811 (1977); **45**, 899 (1977)].
- [15] C. W. Misner, K. S. Thorne, and J. A. Wheeler, *Gravitation* (Freeman, New York, 1973).
- [16] L. S. Brown and G. J. Maclay, *Phys. Rev.* **184**, 1272 (1969).
- [17] R. C. Tolman and P. Ehrenfest, *Phys. Rev.* **36**, 1791 (1930).
- [18] H. M. Haggard and C. Rovelli, *Phys. Rev. D* **87**, 084001 (2013).
- [19] M. Bordag, U. Mohideen, and V. M. Mostepanenko, *Phys. Rep.* **353**, 1 (2001); M. Bordag, *J. Phys. A* **39**, 6173 (2006).
- [20] F. Chen, G. L. Klimchitskaya, V. M. Mostepanenko, and U. Mohideen, *Opt. Express* **15**, 4823 (2007); *Phys. Rev. B* **76**, 035338 (2007); A. A. Banishev, C.-C. Chang, R. Castillo-Garza, G. L. Klimchitskaya, V. M. Mostepanenko, and U. Mohideen, *Phys. Rev. B* **85**, 045436 (2012).
- [21] G. Bimonte, E. Calloni, G. Esposito, L. Milano, and L. Rosa, *Phys. Rev. Lett.* **94**, 180402 (2005).
- [22] G. Bimonte, E. Calloni, G. Esposito, and L. Rosa, *Nucl. Phys.* **B726**, 441 (2005).
- [23] M. Tinkham, *Phys. Rev.* **129**, 2413 (1963).
- [24] G. Bimonte, D. Born, E. Calloni, G. Esposito, U. Huebner, E. Il'ichev, L. Rosa, F. Tafuri, and R. Vaglio, *J. Phys. A* **41**, 164023 (2008); A. Allocca, G. Bimonte, D. Born, E. Calloni, G. Esposito, U. Huebner, E. Il'ichev, L. Rosa, and F. Tafuri, *J. Supercond. Novel Magn.* **25**, 2557 (2012).
- [25] G. Barton, *J. Phys. A* **38**, 2997 (2005).
- [26] A. Kempf, *J. Phys. A* **41**, 164038 (2008).
- [27] T. Accadia, F. Acernese, and M. Alshourbagy, *JINST* **7**, P03012 (2012).
- [28] J. Abadie *et al.* (LIGO Sci Collaboration, Virgo Collaboration), *Phys. Rev. D* **85**, 122007 (2012).
- [29] J. Aasi *et al.*, *Nat. Photonics* **7**, 613 (2013).
- [30] S. Braccini *et al.*, *Astropart. Phys.* **23**, 557 (2005).
- [31] H. Grote, K. Danzmann, K. L. Dooley, R. Schnabel, J. Slutsky, and H. Vahlbruch, *Phys. Rev. Lett.* **110**, 181101 (2013).
- [32] Y. Aso, Y. Michimura, K. Somiya, M. Ando, O. Miyakawa, T. Sekiguchi, D. Tatsumi, and H. Yamamoto (KAGRA Collaboration), *Phys. Rev. D* **88**, 043007 (2013).
- [33] T. Accadia *et al.* (Virgo Collaboration), *Classical Quantum Gravity* **28**, 114002 (2011).
- [34] H. Harry for the (LIGO collaboration), *Classical Quantum Gravity* **27**, 084006 (2010).
- [35] B. Sathyaprakash *et al.*, *Classical Quantum Gravity* **29**, 124013 (2012).
- [36] T. Corbitt, Y. Chen, F. Khalili, D. Ottaway, S. Vyatchanin, S. Whitcomb, and N. Mavalvala, *Phys. Rev. A* **73**, 023801 (2006).
- [37] M. Evans, Optickle LIGO Document Report No. T070260, 2007.
- [38] S. Hild, S. Chelkowski, A. Freise, J. Franc, N. Morgado, R. Flaminio, and R. De Salvo, *Classical Quantum Gravity* **27**, 015003 (2010).
- [39] J. Harms, B. J. J. Slagmolen, R. X. Adhikari, M. Coleman Miller, M. Evans, Y. Chen, H. Müller, and M. Ando, *Phys. Rev. D* **88**, 122003 (2013).
- [40] A. Cavalleri, G. Ciani, R. Dolesi, M. Hueller, D. Nicolodi, D. Tombolato, P. J. Wass, W. J. Weber, S. Vitale, and L. Carbone, *Classical Quantum Gravity* **26**, 094012 (2009).
- [41] J. Wiedersich, S. V. Adichtchev, and E. Rössler, *Phys. Rev. Lett.* **84**, 2718 (2000).
- [42] S. Rowan *et al.*, *Proc. SPIE Int. Soc. Opt. Eng.* **4856**, 292 (2003).
- [43] K. Kuroda and the (LCGT Collaboration), *Classical Quantum Gravity* **23**, S215 (2006).
- [44] R. De Rosa, L. Di Fiore, F. Garufi, A. Grado, A. La Rana, and L. Milano, *Astropart. Phys.* **34**, 394 (2011).
- [45] W. Zimmermann, E. H. Brandt, M. Bauer, E. Seider, and L. Genzel, *Physica (Amsterdam)* **183C**, 99 (1991); see also A. J. Berlinsky, C. Kallin, G. Rose, and A. C. Shi, *Phys. Rev. B* **48**, 4074 (1993).
- [46] E. Bonjour, R. Calemczuk, J. Y. Henry, and A. F. Khoder, *Phys. Rev. B* **43**, 106 (1991).